To appear in the Proc. IEEE BTAS, 2013

LFIQ: Latent Fingerprint Image Quality

Soweon Yoon, Kai Cao, Eryun Liu, and Anil K. Jain *
Department of Computer Science and Engineering,
Michigan State University, East Lansing, MI, U.S.A.
{yoonsowo,kaicao,liueryun,jain}@cse.msu.edu

Abstract

Latent fingerprint images are typically obtained under non-ideal acquisition conditions, resulting in incomplete or distorted impression of a finger, and ridge structure corrupted by background noise. This necessitates involving latent experts in latent fingerprint examination, including assessing the value of a latent print as forensic evidence. However, it is now generally agreed that human factors (e.g., human visual perception, expertise of latent examiners, workload, etc.) can significantly affect the reliability and consistency of the value determinations made by latent examiners. We propose an objective quality measure for latent fingerprints, called Latent Fingerprint Image Quality (LFIQ), that can be effectively used to distinguish latent fingerprints of good quality, which do not require any human intervention, and to compensate for the subjective nature of value determination by latent examiners. We investigate several factors that determine the latent quality: (i) ridge quality based on ridge clarity and connectivity of good ridge structures, (ii) minutiae reliability based on a minutiae dictionary learnt from high quality minutia patches, and (iii) position of the finger by detecting a reference point. The proposed LFIQ metric is based on triangulation of minutiae incorporating the above three factors. Experimental results show that (i) the proposed LFIQ is a good predictor of the latent matching performance by AFIS and (ii) it is also correlated with value determination by latent examiners.

1. Introduction

With the advent of fingerprints for identifying and tracing habitual criminals by the Scotland Yard Police in the early 1900s, fingerprint recognition has become one of the most commonly practiced approaches for human identification in law enforcement and forensics. *Latent* fingerprints refer to the fingerprints obtained by lifting the residues of the finger skin from the surface of objects in contact; those fingerprints found at crime scenes play an important role in solving the crimes. As the residues from finger skin generally deteriorate over time and latent fingerprints often contain only a partial friction ridge structure of the finger, the quality of the latent fingerprints can be poor and the amount of ridge information contained in the latents is typically limited. As a result, while exemplar[1] search (tenprint-to-tenprint matching) can essentially be executed in a fully automated manner using Automated Fingerprint Identification Systems (AFIS), latent search (latent-to-tenprint matching) still requires significant effort by latent examiners, particularly in feature markup and identity determination.

Latent examiners commonly follow the ACE-V methodology [6] to identify latent fingerprints. This methodology consists of the following four phases: (i) *Analysis* phase to determine the value of a latent as one of three levels: Value for Individualization (VID), Value for Exclusion Only (VEO), or No Value (NV); (ii) *Comparison* phase to assess similarity or dissimilarity between the latent which is determined as either VID or VEO and a set of exemplar fingerprints retrieved by AFIS; (iii) *Evaluation* phase to make one of the three identification decisions for each pair of the latent and an exemplar print (i.e., individualization, exclusion, or inconclusive); and (iv) *Verification* phase where a second examiner processes the latent independently and confirms the decision of the first examiner.

One of the critical decisions made by latent examiners is the latent value determination in the analysis phase of the ACE-V protocol. If a latent is determined as NV, it is not processed further for comparison. However, the value determination by latent examiners may not always be reliable or consistent because (i) subjectivity of human visual perception in determining image quality or bias from prior knowledge of the case can affect their decision [17], (ii) different examiners with various levels of expertise in latent examination may not coincide in value determination of the

*This research was supported by a grant from the NSF Center for Identification Technology Research (CITeR).

[1]Exemplar fingerprints refer to rolled and plain fingerprints, which are generally acquired in an attentive mode.

Table 1. The number of latents in each value category and identification rate (rank-1 and rank-100) for each category.

	Value for Individualization (VID)	Value for Exclusion Only (VEO)	No Value (NV)
NIST SD27[a]	210	41	7
WVU	370	74	5
Rank-1 Identification Rate	491 (85%)	46 (40%)	1 (8%)
Rank-100 Identification Rate	525 (91%)	72 (63%)	7 (58%)

[a] The latent examiners' value determination on NIST SD27 is obtained from the study in [12].

same latent print [20, 21], and (iii) heavy workload faced by the examiners in latent print units can lead to insufficient amount of time for analysis which can result in false decisions on latent value [15].

The relationship between latent value determination by examiners and latent identification accuracy by AFIS is shown in Table 1. Two sources of latent fingerprint images along with their value determinations by examiners are evaluated in this paper: 258 latent fingerprints from NIST SD27 [1] and 449 latents from WVU latent database [24]. Three different AFIS were used to search the latents against an exemplar database containing 31,997 rolled fingerprints with both proprietary features from the AFIS and markup features provided by latent examiners. If any one of the three AFIS is able to retrieve the true mate of a latent within rank m, the latent is deemed to be identifiable at rank m. It is noteworthy that a large number of VEO latents can be identified at rank 100 (63%) as well as at rank 1 (40%); 1 out of 12 NV latents is identified at rank 1, and 7 out of 12 NV latents are identified at rank 100. This implies that, while the identification accuracy of AFIS is highly correlated with the value determination by latent examiners, a significant number of VEO or NV latents can still be identified by AFIS.

In exemplar search scenarios, fingerprint image quality is affected by (i) intrinsic factors: saliency of friction ridge structure or dryness/wetness of finger skin, and (ii) extrinsic factors: sensitivity of the fingerprint imaging sensor or positioning of the finger on the sensor. Most algorithms for tenprint quality assessment utilize (i) local properties (e.g., local ridge quality in terms of clarity, orientation, and frequency) and (ii) global properties (e.g., continuity of orientation field or energy concentration in the frequency domain over the entire fingerprint) [5]. As an example, NIST Fingerprint Image Quality (NFIQ) is based on the size of foreground region, the total number of minutiae, minutiae count at different minutiae quality levels, and the size of the fingerprint region at different ridge quality levels [19].

Defining a quality metric for fingerprint images is a challenging problem due to the following reasons. Fingerprint image quality as a predictor of matching accuracy of AFIS is not always correlated to perceptual image quality which is generally defined by sharpness, contrast, noise level, etc. Instead, it is based on the sufficiency of reliable features that can be effectively used in fingerprint matching. As a result, a fingerprint quality metric typically is associated with a certain sensor or a matcher. The NFIQ, a commonly adopted fingerprint quality metric, was developed to overcome the interoperability issue among various sensors and matchers from different vendors. The development of NFIQ 2.0 [9] is underway to reflect the advances in fingerprint matching technology over the past 10 years and update the features and properties of NFIQ. Nevertheless, all existing fingerprint quality measures were designed for rolled or plain fingerprints.

For latent fingerprint images, various extrinsic factors, in addition to intrinsic factors, affect the fingerprint image quality: (i) the surface where the latent print is left can introduce severe background noise in the acquired image, (ii) the latent print may contain impression of only the side or tip of a finger, and (iii) a severe skin distortion can be introduced during impression formation. Hence, a quality measure for latent fingerprints needs to take into account the following considerations:

- Ridge quality in the presence of background noise: Given that latent images often have cluttered background, friction ridge pattern needs to be properly localized in the image, and separated from any overlapping structured background.

- Spatial characteristic of good ridge quality regions: Local ridge areas of good quality that are spatial neighbors tend to have a greater possibility to be matched with the mate than good quality regions that are sparsely distributed.

- Reliability of minutiae: Minutiae are the most critical features in latent matching. Given the relatively small number of minutiae in latents, even a few false minutiae can degrade the latent matching accuracy dramatically. Thus, it is necessary to estimate minutiae reliability in latents.

- Finger position: A latent image that contains only the tip or side of a finger is less likely to be matched with its true mate in an exemplar database which mostly contains the central part of the fingers.

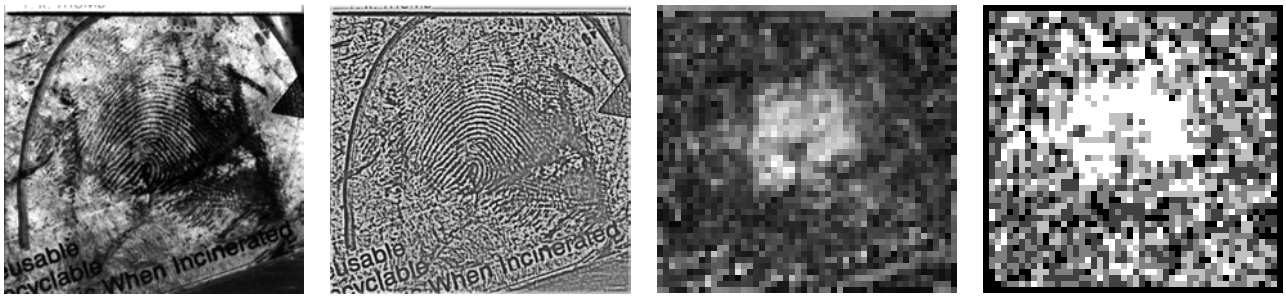

(a) (b) (c) (d)

Figure 1. The amplitude map ($\mathbf{R_A}$) and ridge continuity map ($\mathbf{R_C}$) of the dominant ridge components of a latent image. (a) A latent in NIST SD27 (G065), (b) contrast-enhanced latent image (I^*), (c) amplitude map ($\mathbf{R_A}$), and (d) ridge continuity map ($\mathbf{R_C}$).

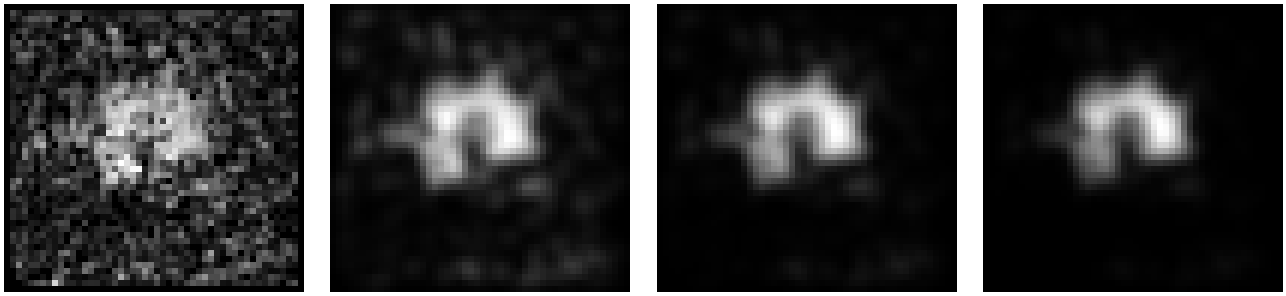

(a) (b) (c) (d)

Figure 2. Ridge quality maps of the latent shown in Fig. 1(a) at different iterations. (a) $\mathbf{Q_R^{(0)}}$, (b) $\mathbf{Q_R^{(2)}}$, (c) $\mathbf{Q_R^{(4)}}$, and (d) $\mathbf{Q_R^{(6)}}$.

In this paper, our goal is to define a quality measure for latent fingerprints, namely Latent Fingerprint Image Quality (LFIQ), which can be used as a predictor of latent matching performance. Our preliminary study on latent fingerprint quality [25] developed a latent quality measure by multiplying the average ridge clarity and minutiae count. We extend the latent quality measure in [25] by incorporating (i) the connectivity of good ridge quality regions at global level, (ii) reliability of minutiae, and (iii) estimation of finger position for computing the LFIQ. Our experimental results show that the proposed LFIQ has a high correlation with latent matching accuracy; latents with high LFIQ value have their true mates retrieved at rank 1 with high probability. Note that, considering that the matching performances of different AFIS for a given latent query can be very different, we determine the value of a latent in a matcher-independent manner; if any of the three AFIS used here can successfully match the latent, we expect its LFIQ score to be high.

2. Features for Defining LFIQ

We consider the following three factors that affect the quality of latent fingerprints: (i) ridge quality, (ii) minutiae reliability, and (iii) finger position. The ridge quality is determined by local ridge clarity and the connectivity of the friction ridge areas with high ridge clarity. The minutia reliability is measured as its likelihood of being a genuine minutia. The position of a finger is estimated by detecting the reference point of a finger (e.g., core point(s) or the maximum curvature point for arch-type fingerprints); minutiae in the central parts of the finger are assigned high weights in LFIQ computation.

2.1. Ridge Quality

The ridge quality of a local block is measured not only by the ridge clarity of the block but also by the ridge continuity with its neighboring blocks [25]. The local ridge quality is propagated over the entire image to determine the ridge connectivity at the global level.

1. Preprocessing: Given a latent image I, its contrast is enhanced by [11, 25]:

$$I^* = \text{sign}(I - \bar{I}) \times \log(1 + |I - \bar{I}|), \qquad (1)$$

where I^* is the enhanced image, $\bar{I}$ is the smoothed image of I by applying a 15×15 averaging filter, and $\text{sign}(x) = 1$ if $x > 0$, otherwise $\text{sign}(x) = -1$. Fig. 1(b) shows the contrast-enhanced image of Fig. 1(a).

2. Dominant Ridge Component Selection: For each 32×32 pixel block in the enhanced image I^* centered at $[m, n]$, the 64×64 subimage is constructed by zero-padding to get high frequency resolution in the Fourier domain. The local amplitude maximum at (u_0, v_0) within the frequency range of $\left[\frac{1}{16}, \frac{1}{5}\right]$ is selected as the dominant ridge component [14, 25]. Let a_{mn}, f_{mn}, and θ_{mn} denote the amplitude, frequency, and direction of the dominant ridge component of the block at $[m, n]$. The amplitude map is defined as $\mathbf{R_A}[m, n] = a_{mn}$ (see Fig. 1(c)).

3. Ridge Continuity: The adjacent blocks in a 4-connected neighborhood are continuous if the following three conditions are satisfied [14, 25]:

$$\text{(i) } \min\{|\theta_1, \theta_2|, \pi - |\theta_1, \theta_2|\} \leq T_\theta,$$
$$\text{(ii) } \left|\frac{1}{f_1} - \frac{1}{f_2}\right| \leq T_f, \text{ and}$$
$$\text{(iii) } \frac{1}{16} \sum_{(x,y)\in\mathcal{L}} |L_1(x, y) - L_2(x, y)| \leq T_p, \quad (2)$$

where $\mathcal{L}$ denotes the set of 16 pixels on the border of the two adjacent blocks, and $L_i(x, y)$ is the filtered image of the block i by a directional bandpass filter with parameters θ_i and f_i [18]. The three thresholds, T_θ, T_f, and T_p, are set to $\frac{\pi}{10}$, 3, and 0.6, respectively. The local ridge continuity of a block at $[m, n]$, $\mathbf{R_C}[m, n]$, is defined as the number of neighboring blocks that are continuous with respect to the central block (see Fig. 1(d)).

4. Ridge Quality: To reflect the ridge connectivity at the global level, a ridge quality map is constructed by propagating the amplitude and ridge continuity maps iteratively. The initial ridge quality map, $\mathbf{Q_R^{(0)}}[m, n]$, is defined as $\mathbf{R_A}[m, n] \cdot \mathbf{R_C}[m, n]$. The ridge quality map is updated by:

$$\mathbf{Q_R^{(k)}}[m, n] = \mathbf{Q_R^{(k-1)}}[m, n] + \sum_{\substack{[m',n'] \\ \in\mathcal{C}[m,n]}} \mathbf{Q_R^{(k-1)}}[m', n'],$$

where $\mathcal{C}$ is the set of neighboring blocks that are continuous with respect to the block at $[m, n]$, followed by filtering $\mathbf{Q_R^{(k)}}[m, n]$ with a 3×3 averaging filter. The number of iterations is set to 6 (i.e., $\mathbf{Q_R} = \mathbf{Q_R^{(6)}}$). Fig. 2 shows the ridge quality maps at different iterations.

2.2. Minutiae Reliability

Even if the ridge quality is determined to be high in a local area, the reliability of a minutia located in the area may not be high since the ridge quality does not necessarily measure the *fingerprint* ridge quality; it can, for example, measure the strength of the structured background noise. Based on the minutiae dictionary learnt from a set of high quality minutia patches in exemplar fingerprints, the structural similarity between an image patch around a minutia and the minutiae dictionary defines the reliability of the minutia.

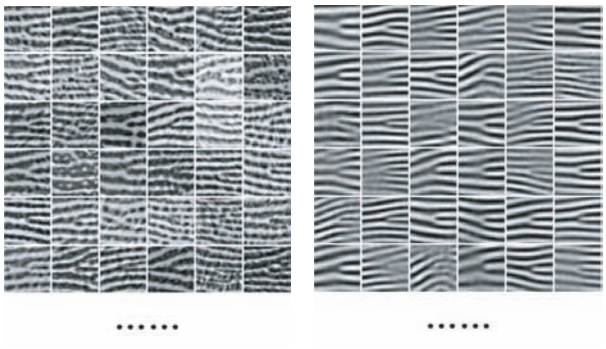

(a) (b)

Figure 3. Minutiae dictionary learning. (a) Minutia patches used for training and (b) minutiae dictionary elements.

2.2.1 Minutiae Dictionary Learning

A large number of high quality minutia patches extracted from a subset of NIST SD4 [2] are used to learn the minutiae dictionary in the following way:

1. High quality fingerprint images with NFIQ values of 1, 2 or 3 are selected.

2. Minutiae are extracted by a commercial-off-the-shelf (COTS) fingerprint matcher.

3. If a minutia is located in a block with the highest ridge quality as indicated by NBIS [23] (i.e., quality level of 4), the 48×48 image patch centered at the minutia and aligned along the minutia direction is cropped.

4. All the minutia patches are normalized to images with a mean of 0 and a standard deviation of 1.

In total, 20,000 minutia patches are used to form a training set for minutiae dictionary learning. Fig. 3(a) shows some examples of high quality minutia patches used for the minutiae dictionary learning. The minutiae dictionary, D, with 128 elements is learnt from the training set via K-SVD algorithm [4]. Some of the minutiae dictionary elements are shown in Fig. 3(b).

2.2.2 Minutia Reliability Measure

The reliability of a minutia in a latent is defined as the structural similarity [22] between the minutia patch and its closest dictionary element. For a normalized minutia patch p,

which is centered at the minutia and aligned along the minutia direction, the minutia reliability is obtained by:

$$Q_M = \max SSIM(p, D), \tag{3}$$

where

$$SSIM(p,d) = \frac{(2\mu_p\mu_d + C_1)(2\sigma_{pd} + C_2)}{(\mu_p^2 + \mu_d^2 + C_1)(\mu_p^2 + \mu_d^2 + C_2)}, \tag{4}$$

d is an element in the minutiae dictionary D, μ_i and σ_i are the mean and standard deviation of the image patch i, σ_{pd} is the correlation coefficient between p and d, and C_1 and C_2 are constants.

2.3. Position of Finger

Since most of the exemplar fingerprints typically contain the central part of a finger, a latent with central part of a finger is more likely to be matched with its true mate. The reference point of a latent is determined based on the orientation field reconstructed from the minutiae; high weights are assigned to the minutiae located in the central part of the finger and low weights are assigned to the minutiae far from the center of the finger.

2.3.1 Orientation Field Reconstruction

The orientation field of a latent is reconstructed based on minutiae with high reliability [10]. The local ridge orientation at a block $[m, n]$, $D_c[m, n]$, is estimated by selecting the nearest minutia in each of the 8 sectors and then by summing the doubled directions of the selected minutiae:

$$D_c[m,n] = \tan^{-1}\left(\frac{v}{u}\right),$$

$$u = \sum_k \cos(2\theta_k)w_k,\ v = \sum_k \sin(2\theta_k)w_k, \tag{5}$$

where θ_k is the direction of the selected minutia in the sector k, and w_k is a weighting function (the reciprocal of the Euclidean distance between the block center and the minutia). The orientation field $\theta[m, n]$ is computed as $D_c[m, n]/2$.

2.3.2 Reference Point Detection

The reference point of a fingerprint is defined as the point where the curvature of convex ridge structure is the maximum [26]. To measure the curvature of the ridge structure, a complex filter T_c is applied to the reconstructed orientation field:

$$T_c = (x + iy)g_\sigma(x, y), \tag{6}$$

where $g_\sigma(x, y)$ is a 2-dimensional Gaussian function with a standard deviation of σ. The complex filter T_c can essentially characterize the orientation field around a core, and has been used to detect cores [16] and reference points [7].

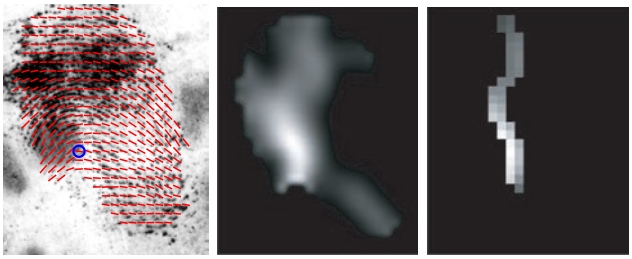

(a) (b) (c)

Figure 4. Reference point detection. (a) Reconstructed orientation field from reliable minutiae, (b) curvature map ($\hat{C}$), and (c) curvature values along the connected convex ridge points in vertical direction (PC). The detected reference point is indicated in (a) as a circle.

The filter response C is obtained by convolving the conjugate of the complex filter T_c and the orientation tensor $z = \cos(2\theta) + i\sin(2\theta)$, where θ is the orientation field. To measure the *convex* curvature of the ridge structure, C is projected onto the $\pi/2$ direction, equivalent to taking the imaginary part of C:

$$\hat{C} = Im\{C\}. \tag{7}$$

To reliably determine the reference point from the curvature map $\hat{C}$, the convex ridge points in each row are detected and their connectivity in vertical direction is examined. The convex ridge points in a row satisfy the following conditions: (i) $|\theta(x, y)| < \theta_T$, where $\theta_T = \frac{\pi}{6}$, (ii) $\theta(x-1, y) < 0$, and (iii) $\theta(x+1, y) > 0$. A binary map indicating the location of convex ridge points is constructed: $P(x, y) = 1$ when a convex ridge point is at (x, y); otherwise, $P(x, y) = 0$. The connectivity of the convex ridge points in vertical direction is computed [8]: for (x, y) such that $P(x, y) = 1$,

$$PC(x,y) = \begin{cases} 1, \text{ if } y = 1 \\ 1, \text{ if } \sum_{z=x-1}^{x+1} P(z, y-1) = 0 \\ \sum_{z=x-1}^{x+1} P(z, y-1), \text{ otherwise.} \end{cases} \tag{8}$$

Finally, a point at (x_o, y_o) is determined as a reference point if (i) the curvature $\hat{C}$ is maximum at (x_o, y_o) along the connected convex ridge points in the vertical direction and (ii) $\hat{C}(x_o, y_o) > T_C$ and $PC(x_o, y_o) > T_{PC}$, where $T_C = 0.4$ and $T_{PC} = 7$. Fig. 4 illustrates reference point detection.

3. Latent Quality Score Computation

Given a set of minutiae in a latent fingerprint, the Delaunay triangulation is constructed (see Fig. 5). For a triangle T_i consisting of minutiae M_{ij}, $j = 1, 2, 3$ at its vertices, the

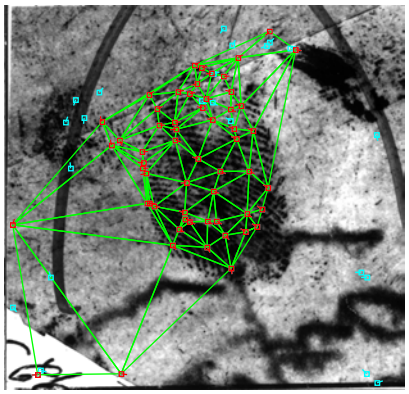

Figure 5. The Delaunay triangulation with reliable minutiae shown in red.

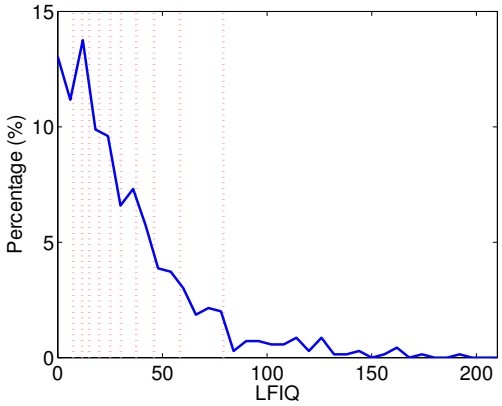

Figure 6. Histogram of LFIQ values for 707 latents in the experiments. The red dotted lines indicate the median LFIQ scores for the quality indices 10, 20, ..., 100.

quality score of the triangle is computed by:

$$Q_{T_i} = Q_{R_i} \sum_{j=1}^{3} Q_{M_{ij}} W_{M_{ij}}, \text{ for } M_{ij} \text{ such that } Q_{M_{ij}} > T_{QM} \tag{9}$$

where Q_{R_i} is the average ridge quality in T_i, $Q_{M_{ij}}$ is the reliability of the minutia M_{ij} such that $Q_{M_{ij}} > T_{QM}$, $T_{QM} = 0.3$, and $W_{M_{ij}}$ is the weight based on the distance between the minutia and the reference point of the latent (if it exists). The weight function is set to a 2-dimensional Gaussian where the mean is located at the reference point.

LFIQ score for a given latent is defined as:

$$LFIQ = \sum_{i=1}^{N} Q_{T_i}, \tag{10}$$

where N is the number of the Delaunay triangles in the latent image.

4. Experimental Results

Latent fingerprints from two databases are used in our evaluation of LFIQ: (i) 258 latents from NIST SD27 [1] and (ii) 449 latents from WVU latent database [24]. An exemplar database contains 31,997 rolled fingerprints: (i) 258 mated rolled prints in NIST SD27, (ii) 449 mated rolled prints in WVU latent database, (iii) 4,290 rolled prints in WVU database, and (iv) 27,000 rolled prints in NIST SD14 [3]. Three COTS fingerprint matchers (one latent fingerprint matcher and two tenprint fingerprint matchers) are used to search the latents against the exemplar database. Proprietary features from the matchers and markup minutiae are input to the matchers.

Fig. 6 shows the histogram of LFIQ values for the 707 latents used in our experiments. The LFIQ scores are quantized into 100 bins such that each bin contains 100 latents and a window for binning slides with a fixed step size. The red dotted lines in Fig. 6 indicate the median LFIQ scores for the bins labeled as quality indices of 10, 20, ..., 100. Fig. 7 shows examples of latents corresponding to some of these quality indices. Note that a high quality index refers to high LFIQ score.

The proposed LFIQ is compared to the latent quality measure proposed in [25]. To show the utility of new features used in the proposed LFIQ (i.e., global connectivity of good ridge quality regions, minutiae reliability, and finger position), the minutiae set for predicting LFIQ is constructed by combining manually marked minutiae and proprietary minutiae sets from the two tenprint matchers; this augmented set contains both reliable and unreliable minutiae. Fig. 8 shows the rank-1 identification rate of latents with respect to quality index. For each quality index bin, the percentage of latents whose mates are retrieved at rank 1 is used as an evaluation criterion. A high identification accuracy is expected for latents with high quality indices. Note that, by fusing the results from the three different COTS matchers and using both proprietary minutiae and markup minutiae, 72% of the latents can be identified at rank 1. Fig. 8 also shows the ideal performance when the exact retrieval ranks of the true mates are available. The minutiae count used in [25] is not a good feature for latent quality estimation in the presence of unreliable minutiae. The proposed LFIQ effectively utilizes the minutiae reliability measure and finger position estimation to determine the latent quality compared to [25].

To compare the proposed LFIQ with an AFIS tenprint quality measure, we first mask out the background region in the latent to reduce the interference of the background noise in quality estimation. For a fair comparison, the LFIQ also used the proprietary minutiae from the matcher. The LFIQ gave comparable results to the tenprint quality measure without knowing the internal details of the matcher.

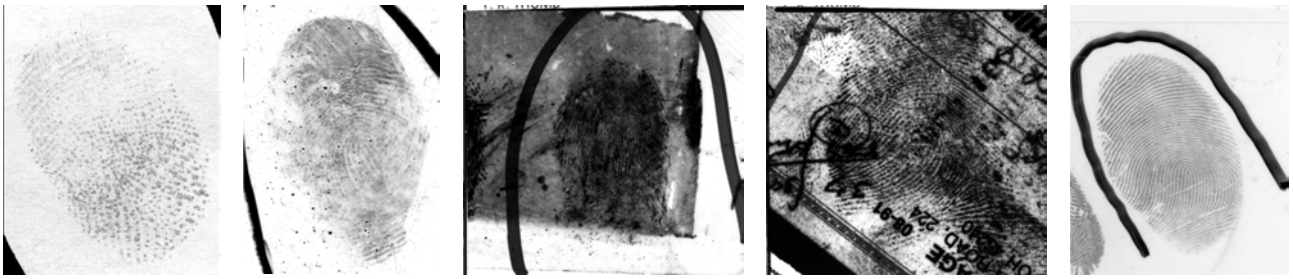

(a) (b) (c) (d) (e)

Figure 7. Latent images corresponding to quality indices of (a) 1 (lowest quality), (b) 30, (c) 50, (d) 80, and (e) 100 (highest quality).

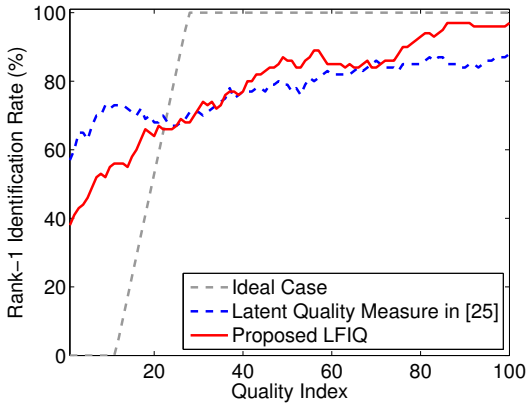

Figure 8. Rank-1 identification rate with respect to different quality measures: (i) ideal case where the rank of the true mate is known, (ii) the latent quality measure in [25], and (iii) the proposed LFIQ.

(a) U254, NIST SD27

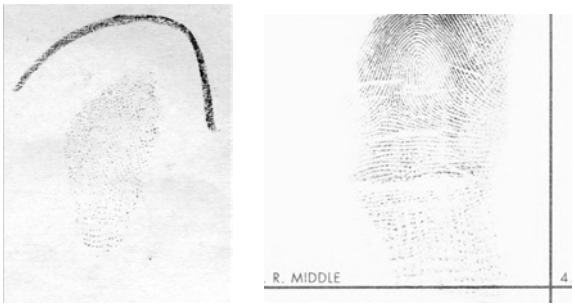

(b) W803S03, WVU

Figure 9. Latents and mated rolled prints for which the proposed LFIQ correctly predicts the AFIS performance. (a) Latent with high quality index of 96; determined as NV by examiners, but the retrieval rank of the true mate by AFIS is 1; and (b) latent with low quality index of 1; determined as VID by examiners, but the retrieval rank of the true mate by AFIS is 2,349.

We also evaluated the proposed LFIQ for estimating tenprint quality. We used 1,844 rolled fingerprint pairs in NIST SD4[2] [2] and compared the LFIQ to the AFIS tenprint quality measure and the NFIQ [19]. Again, the proposed LFIQ showed a comparable result to the two tenprint quality measures.

The proposed LFIQ is correlated with the value determination by latent examiners. The mean LFIQ index of the latents determined as VID by examiners was 58 (upper quartile and lower quartile were 85 and 34, respectively) while the mean LFIQ index of the VEO latents was 20 (upper quartile and lower quartile were 30 and 2, respectively) and that of the NV latents was 21 (upper quartile and lower quartile were 26 and 1, respectively). This implies that the proposed LFIQ generally agrees to the examiners' value determination on latent fingerprints.

Fig. 9 shows examples where the proposed LFIQ can successfully predict latent value unlike the subjective evaluation of latent examiners. Fig. 10 shows a latent for which both the proposed LFIQ and the value determination by examiners indicate that it is of good quality, yet the true mate is retrieved only at a rank of 600.

[2]We excluded those images used for minutiae dictionary learning.

5. Summary

Fingerprint quality assessment primarily aims to predict the matching performance of AFIS to ensure the reliability of matching results. By rejecting poor quality fingerprints, an AFIS can reduce incidents of false accepts or false rejects. While a number of fingerprint quality measures have been developed for rolled and plain fingerprints,

Figure 10. A latent (W944F08, WVU) and mated rolled print for which the proposed LFIQ is high (93); latent examiners determine the latent as VID, but the mate is retrieved at rank 600.

very little effort has been made to devise a latent fingerprint quality measure. Reliable latent quality assessment is crucial, primarily to prevent any evidence of value from being discarded. Recent studies [20, 21] and evaluations of latent matchers [13] show that latent value determination by examiners can be subjective and inconsistent, which motivates us to develop an objective measure of latent quality. We have proposed a latent quality metric, called LFIQ, that incorporates ridge quality, minutiae reliability, and finger position in latent image. The proposed LFIQ satisfies desirable properties of a latent quality measure: (i) it can predict the matching performance by AFIS with high accuracy and (ii) it is highly correlated with value determination by latent examiners. The proposed LFIQ can be used to (i) distinguish high quality latents that do not need any human intervention and can be identified in "lights-out" mode, and (ii) assist latent examiners in their value determination for latent fingerprints.

References

[1] NIST Special Database 27: Fingerprint Minutiae from Latent and Matching Tenprint Images. http://www.nist.gov/srd/nistsd27.cfm.

[2] NIST Special Database 4: NIST 8-Bit Gray Scale Images of Fingerprint Image Groups (FIGS). www.nist.gov/srd/nistsd4.cfm.

[3] NIST Special Database 14: NIST Mated Fingerprint Card Pairs 2 (MFCP2). www.nist.gov/srd/nistsd14.cfm.

[4] M. Aharon, M. Elad, and A. Bruckstein. K-SVD: An Algorithm for Designing Overcomplete Dictionaries for Sparse Representation. *IEEE Trans. on Signal Processing*, 54(11):4311–4322, 2006.

[5] Alonso-Fernandez et al. A Comparative Study of Fingerprint Image-Quality Estimation Methods. *IEEE Trans. Information Forensics and Security*, 2(4):734–743, 2007.

[6] D. R. Ashbaugh. *Quantitative-Qualitative Friction Ridge Analysis: An Introduction to Basic and Advanced Ridgeology*. CRC Press, 1999.

[7] K. Cao, J. Liang, and J. Tian. A Div-Curl Regularization Model for Fingerprint Orientation Extraction. In *Proc. Biometrics: Theory, Applications and Systems*, pages 231–236, 2012.

[8] K. C. Chan, Y. S. Moon, and P. S. Cheng. Fast Fingerprint Verification Using Subregions Of Fingerprint Images. *IEEE Trans. on Circuits and Systems for Video Technology*, 14(1):95–101, 2004.

[9] Development of NFIQ 2.0. http://www.nist.gov/itl/iad/ig/development_nfiq_2.cfm.

[10] J. Feng and A. K. Jain. Fingerprint Reconstruction: From Minutiae to Phase. *IEEE Trans. PAMI*, 33(2):209–223, 2011.

[11] H. Fronthaler, K. Kollreider, and J. Bigun. Local Features for Enhancement and Minutiae Extraction in Fingerprints. *IEEE Trans. on Image Processing*, 17(3):354–363, 2008.

[12] R. A. Hicklin et al. Latent Fingerprint Quality: A Survey of Examiners. *Journal of Forensic Identification*, 61(4):385–419, 2011.

[13] M. Indovina, V. Dvornychenko, R. A. Hicklin, and G. I. Kiebuzinski. Evaluation of Latent Fingerprint Technologies: Extended Feature Sets [Evaluation #2]. NISTIR 7859, 2012.

[14] A. K. Jain and J. Feng. Latent Palmprint Matching. *IEEE Trans. PAMI*, 31(6):1032–1047, 2009.

[15] National Research Council. Strengthening Forensic Science in the United States: A Path Forward, 2009.

[16] K. Nilsson and J. Bigun. Localization of Corresponding Points in Fingerprints by Complex Filtering. *Pattern Recognition Letters*, 24(13):2135–2144, 2003.

[17] NIST and NIJ. Latent Print Examination and Human Factors: Improving the Practice through a Systems Approach, 2012.

[18] B. G. Sherlock, D. M. Monro, and K. Millard. Fingerprint Enhancement by Directional Fourier Filtering. *Visual Image Signal Processing*, 141:87–94, 1994.

[19] E. Tabassi, C. Wilson, and C. Watson. Fingerprint Image Quality. NISTIR 7151, August 2004.

[20] B. T. Ulery, R. A. Hicklin, J. Buscaglia, and M. A. Roberts. Accuracy and Reliability of Forensic Latent Fingerprint Decisions. *Proc. of the National Academy of Sciences*, 108(19):7733–7738, 2011.

[21] B. T. Ulery, R. A. Hicklin, J. Buscaglia, and M. A. Roberts. Repeatability and Reproducibility of Decisions by Latent Fingerprint Examiners. *PLoS ONE*, 7(3), 2012.

[22] Z. Wang, A. C. Bovik, H. R. Sheikh, and E. P. Simoncelli. Image Quality Assessment: From Error Visibility to Structural Similarity. *IEEE Trans. on Image Processing*, 13(4):600–612, 2004.

[23] C. Watson, M. Garris, E. Tabassi, C. Wilson, R. M. McCabe, S. Janet, and K. Ko. NIST Biometric Image Software. www.nist.gov/itl/iad/ig/nbis.cfm.

[24] West Virginia University Latent Fingerprint Database. http://www.cse.msu.edu/~rossarun/.

[25] S. Yoon, E. Liu, and A. K. Jain. On Latent Fingerprint Image Quality. In *Proc. International Workshop on Computational Forensics*, 2012.

[26] A. Yoshida and M. Hara. Fingerprint Image Quality Metrics That Guarantees Matching Accuracy. Biometric Quality Workshop, 2006. http://biometrics.nist.gov/cs_links/quality/workshopI/proc/hara_nec_qualitymetrics.pdf.